

Technical Notes

TECHNICAL NOTES are short manuscripts describing new developments or important results of a preliminary nature. These Notes cannot exceed 6 manuscript pages and 3 figures; a page of text may be substituted for a figure and vice versa. After informal review by the editors, they may be published within a few months of the date of receipt. Style requirements are the same as for regular contributions (see inside back cover).

Behavior of Heavy Particles in an Acoustically Forced Confined Shear Flow

E. J. Chang* and K. Kailasanath†
U.S. Naval Research Laboratory,
Washington, D.C. 20375

Introduction

IN many combustion systems liquid fuel is sprayed into a combustor where it mixes and burns with air. In other applications the fuel may be injected in the form of a slurry or as solid particles in a gaseous stream. In many such situations it may be desirable to actively control the system to obtain conditions that may improve the efficiency of the system through enhanced dispersion and favorable particle distribution.

Typically the physical characteristics of such systems resemble those of a shear flow confined by a complex geometry and particle dynamics in these systems are of extreme interest. Our previous work regarding particle behavior in confined shear flows¹ indicated that the time-dependent dispersion is governed by the characteristic flow frequencies of the system. Preliminary results² for simulations with acoustically forced flow indicated that, indeed, such forcing does increase the dispersion in the system. Wang³ has suggested that injecting in-phase or out-of-phase with characteristic flow frequencies in a free shear layer can act to enhance or inhibit lateral dispersion of particles. Evidence of enhanced dispersion due to phase-coupled injection of particles at low Stokes numbers has been recently observed in the experimental work of Yu et al.⁴ In this Note we present numerical results showing the effect acoustic forcing, as well as phase-coupled particle injection, has on the dispersion and distribution of particles at moderate Stokes numbers [$S = \mathcal{O}(1)$] in a confined system.

Numerical Model

Unsteady flow into a central dump ramjet combustor is computed by solving the compressible, time-dependent, conservative equations for mass, momentum, and energy in an axisymmetric geometry using a conservative, monotonic algorithm with fourth-order phase accuracy, the flux-corrected transport algorithm.⁵ Further details on the numerical methods employed can be found in Chang and Kailasanath.¹ The strengths and limitations of this approach have been presented in detail by Boris et al.⁶ The geometric configuration of the idealized ramjet used is the same as that used in our previous studies,^{1,7} which we found to be converged and accurate using a 60×120 grid and is shown in Fig. 1. A prescribed mean inflow velocity of 100 m/s flows through the inlet with a mass flow rate of 0.78 kg/s and exits through an annular nozzle modeled to produce

choked flow. The initial chamber pressure is 188 kPa and the inlet diameter is $D = 6.35$ cm.

A dilute system consisting of heavy spherical particles in a one-way coupled system is considered. The particles are assumed to be small in comparison with the smallest scales of the flow and the loading such that the presence of the particles does not modify the gas phase flow in the combustor. An assumption of no particle-particle interaction has also been adopted.

A Lagrangian method is used to track each particle. When the density of the particle ρ_p is much larger than the density of the surrounding fluid ρ_f , the equation governing the motion of each particle in the absence of gravity is

$$\frac{d\mathbf{V}(t)}{dt} = \frac{[\mathbf{u}(\mathbf{Y}, t) - \mathbf{V}(t)]f(Re_p)}{\tau_p} \quad (1)$$

where $\mathbf{V}(t)$ and $\mathbf{Y}(t)$ are the velocity and position of the particle; τ_p is the Stokes response time given as $\tau_p = \rho_p d_p^2 / 18\mu$, where d_p is the diameter of the particle and μ is the dynamic viscosity of the surrounding fluid; $\rho_p = \rho_{\text{water}}$ and $\mu = \mu_{\text{air}}$ at one atmosphere of pressure and 288 K are used for the simulations. The Stokes number is given as $S = \tau_p / t_\sigma$, where $t_\sigma = 1/\sigma_y$ and σ_y is the vortex shedding frequency at the combustor step. The coefficient $f(Re_p)$ is a scalar function of the particle Reynolds number $Re_p = |\mathbf{V} - \mathbf{u}|d_p/\nu_{\text{air}}$ and is equal to unity for the Stokes flow assumption of this study. Because particle Reynolds numbers remain small ($Re_p < 1$) for the particle sizes used in this study, the effect of using a nonlinear drag law to calculate $f(Re_p)$ as compared with the linear assumption used here was found to yield small quantitative but no qualitative differences. Similarly, use of different injection locations yield similar results to those presented here.

Particles are injected into the ramjet combustor every $10\Delta t$, where $\Delta t = 0.376 \times 10^{-6}$ s, at the step corner $r_{i0} = D/2$ and $z = 0$ with zero radial velocity and streamwise velocity $v_{\text{inj}} = 50$ m/s, the approximate convected velocity of the large-scale structures in the shear layer in this region of the combustor. A fourth-order predictor-corrector method is used to obtain the particle velocity and location in time, and a two-dimensional sixth-order Lagrangian interpolation scheme is used to interpolate flow properties to the particle locations.

The results presented here are from simulations with absorptive boundary conditions in which a particle is assumed to stick to the combustor wall upon impact and remain fixed at that location for the remainder of the simulation. The results for simulations with specular reflective boundary conditions yield qualitatively similar results.

Results

From our previous work with this flow configuration and conditions^{1,7} we found that, in the absence of flow forcing, vortex

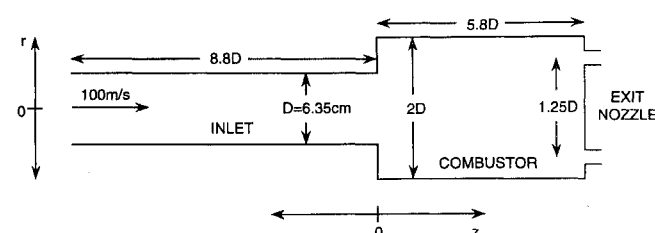


Fig. 1 Schematic of flow configuration.

Received May 1, 1996; revision received July 5, 1996; accepted for publication July 27, 1996; also published in *AIAA Journal on Disc*, Volume 2, Number 1. This paper is declared a work of the U.S. Government and is not subject to copyright protection in the United States.

*Mathematician, Center for Reactive Flow and Dynamical Systems, Laboratory for Computational Physics and Fluid Dynamics, Code 6410.

†Head, Center for Reactive Flow and Dynamical Systems, Laboratory for Computational Physics and Fluid Dynamics, Code 6410. Member AIAA.

shedding at the combustor step occurs at a frequency of $\sigma_s = 1380$ Hz. A second characteristic frequency $\sigma_m = 690$ Hz is also observed, corresponding to the first subharmonic of the vortex shedding frequency and the first merging of vortex structures as they travel downstream. The dominant geometry related acoustic mode of the system is the quarter wave of the inlet (145 Hz).

The dispersion $\delta(t)$ of particles is defined as the rms radial deviation of particle location from the injection location and is given (in centimeters) as

$$\delta(t) = \left[\frac{\sum_{i=1}^{N(t)} [r_i(t) - r_{i0}]^2}{N(t)} \right]^{1/2} \quad (2)$$

where $N(t)$ is the number of particles in the combustor at time t . Particles that have contacted the outer wall are not included in the dispersion measurement. Our previous results¹ indicate that dispersion is maximized at $S \approx 1$.

By examining local dispersion at distinct downstream locations, we found that the shedding frequency σ_s governs the behavior of dispersion in the front region of the combustor, even at locations where the merging frequency characterizes the fluid flow. The vortex merging and acoustic modes are not observed until particles have traveled further downstream with lower frequencies being seen at more distant downstream locations. Thus, the merging frequency σ_m was seen to characterize local dispersion at locations downstream of the actual merging location, the absence of a 690-Hz component at the actual merging location being due to the finite response time of particles to the local fluid flow. The dependence of dispersion on characteristic flow frequencies suggests that acoustic forcing at these frequencies would have a measurable effect on particle dispersion.

Acoustic Forcing and Phase-Coupled Injection

A sinusoidal perturbation is employed, sourced at the exhaust end of the combustor ($z = 5.8D$) with an amplitude of 0.5% of the initial chamber pressure with a frequency of 690, 1380, or 145 Hz, the dominant characteristic frequencies of the system. In addition, simulations were performed with forcing at a frequency unrelated with the system; in this case, at 1000 Hz. The particle size chosen for these calculations is a 15- μm diam ($S = 0.97$), which was found to be optimally dispersed in the unforced case.

An examination of the dispersion as a function of time indicates that in all cases the dispersion rate is increased significantly, with forcing at the shedding frequency having the greatest effect. In the front region of the combustor this is the characteristic frequency in the shear layer and governs the dispersion. The forcing enhances development of the flow structures (vortex shedding) increasing lateral dispersion via larger centrifugal effects.

Simulations were then run where injection occurs in-phase or out-of-phase with the forcing. The injection rate is increased to $5\Delta t$ but occurs only when the pressure perturbation is either positive (in-phase) or negative (out-of-phase). Thus the average injection rate remains the same as in the previous unforced case. Figure 2 shows the dispersion for injecting in-phase and out-of-phase with the forcing frequency. Because particles are injected with approximately the same streamwise velocity as the gas phase in the shear layer, dispersion is increased when injection is in-phase with the forcing as particles travel downstream with the shed vortex structures. Similarly, decreased dispersion is observed when injecting out-of-phase. Here particles are injected "in between" flow structures and centrifugal effects are minimized. Similar results are attained when forcing at the merging frequency.

The time-averaged axial particle distribution $\overline{P_z(t)}$, obtained by taking the average of 10 sets of data sampled over a 75.2-ms period (approximately 104 vortex shedding events) during a simulation run, is shown in Fig. 3. This distribution shows the number of particles for a given axial location as a fraction of the total number of particles in the system. In the unforced case, with continuous injection, a fairly uniform distribution is observed throughout much of the length of the combustor. Forcing the flow, in addition to increasing the dispersion, shifts the particle distribution upstream, increasing the

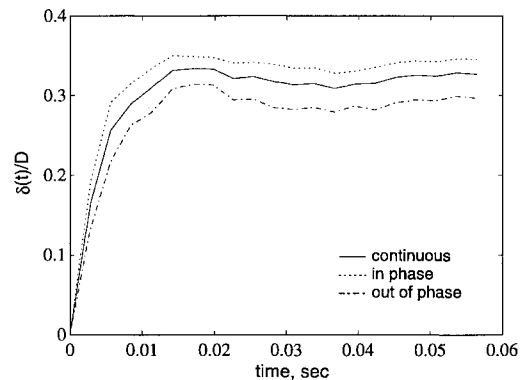


Fig. 2 Dispersion of 15- μm -diam particles ($S = 0.97$) with acoustic forcing at 1380 Hz with continuous injection, injecting in-phase with the forcing and out-of-phase with the forcing frequency.

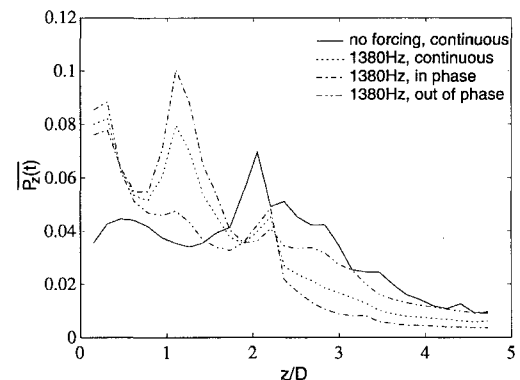


Fig. 3 Time-averaged axial particle distribution for 15- μm -diam particles ($S = 0.97$) with acoustic forcing at 1380 Hz with continuous injection, injecting in-phase with the forcing and out-of-phase with the forcing frequency.

percentage of particles found at the front region of the combustor. This front-weighted distribution is further increased by injecting in-phase with the acoustic forcing. However, injecting out-of-phase has the reverse effect, decreasing the number of particles in the front of the combustor, yielding a more uniform distribution.

Conclusions

Acoustically forcing the flow at the characteristic system frequencies was found to increase the dispersion rate. Forcing at the vortex shedding frequency increases centrifugal effects and was found to have the greatest initial effect. In addition, acoustic forcing had the effect of weighting the axial distribution of particles toward the front of the combustor, this effect being further enhanced when coupled with in-phase particle injection. Conversely, by injecting out-of-phase, centrifugal effects are minimized and particles are allowed to remain in the shear layer for longer periods of time, resulting in a more uniform distribution throughout the combustion chamber. We also note that a heavily front-weighted axial distribution is expected only for optimally sized particles where centrifugal effects are significant enough to achieve high ejection rates from the shear layer. Smaller particles will be carried downstream by the flow and at high Stokes numbers particles may not leave the shear layer until they are well downstream.

For nonuniformly distributed particles in a shear layer, phase-coupled injection of particles was found to affect measured dispersion. Here we found that, for Stokes numbers on the order of unity, injecting in-phase with the forcing acts to increase dispersion due to stronger centrifugal effects, whereas injecting out-of-phase decreases measured dispersion. Note that this result differs from, but does not contradict, low Stokes number results, where enhanced dispersion is due to entrainment of particles into large vortex structures and decreased dispersion is seen when particles are injected into, and remain in, the small core region between structures.

Combined, these results suggest that phase-coupled injection can be used to achieve significantly increased dispersion for all but the largest Stokes numbers where particle trajectories are relatively insensitive to the surrounding carrier phase.

Acknowledgments

This work has been supported by the Mechanics and Energy Conversion Division of the Office of the Naval Research and the Naval Research Laboratory. A grant of high performance computing time from the Department of Defense High Performance Computing Shared Resource Center, U.S. Army Corps of Engineers Waterways Experiment Station, is also gratefully acknowledged.

References

- ¹Chang, E. J., and Kailasanath, K., "Simulations of Particle Dynamics in a Confined Shear Flow," *AIAA Journal*, Vol. 34, No. 6, 1996, pp. 1160–1166.
- ²Chang, E. J., and Kailasanath, K., "Heavy Particles in a Confined High Speed Shear Flow," *Gas-Solid Flows*, ASME-FED Vol. 228, American Society of Mechanical Engineers, New York, 1995, pp. 3–8.
- ³Wang, L. P., "Dispersion of Particles Injected Nonuniformly in a Mixing Layer," *Physics of Fluids A*, Vol. 4, No. 8, 1992, pp. 1599–1601.
- ⁴Yu, K., Wilson, K. J., Parr, T. P., Smith, R. A., and Schadow, K. C., "Characterization of Pulsating Spray Droplets and Their Interaction with Vortical Structure," AIAA Paper 96-0083, Jan. 1996.
- ⁵Boris, J. P., and Book, D. L., "Solution of Continuity Equation by the Method of Flux Corrected Transport," *Methods in Computational Physics*, Vol. 16, Academic, New York, 1976, pp. 85–129.
- ⁶Boris, J. P., Grinstein, F. F., Oran, E. S., and Kolbe, R. L., "New Insights into Large Eddy Simulation," *Fluid Dynamics Research*, Vol. 10, Dec. 1992, pp. 199–228.
- ⁷Kailasanath, K., Gardner, J. H., Oran, E. S., and Boris, J. P., "Numerical Simulations of High-Speed Flows in an Axisymmetric Ramjet," AIAA Paper 88-0339, Jan. 1988.

Transition Correlation in Flow over a Swept Cylinder

J. A. Masad*

High Technology Corporation,
Hampton, Virginia 23666

Introduction

THE transition process in boundary-layer flow over a highly swept cylinder is dominated by the crossflow instability. It is of practical interest to have an analytical correlation of transition location in low-speed flow over a swept cylinder with parameters such as freestream Reynolds number and sweep angle. In this work, we develop such an analytical correlation, based on the extensive experimental data of Poll.¹

Analytical Correlation

The experiment of Poll was performed on a faired cylinder with a chord length of $c^* = 457$ mm, which is equal to 4 times the radius R^* ($c^* = 4R^*$); therefore, $R^* = 114$ mm. The experiment was performed at low speed, and the freestream Reynolds number Re varied from 0.22×10^6 to 0.42×10^6 , where Re is defined as

$$Re = \frac{Q_\infty^* R^*}{\nu^*}$$

Received May 11, 1995; revision received April 30, 1996; accepted for publication July 29, 1996; also published in *AIAA Journal on Disc*, Volume 2, Number 1. Copyright © 1996 by the American Institute of Aeronautics and Astronautics, Inc. All rights reserved.

*Research Scientist, 28 Research Drive; currently Senior Engineer, Lockheed Martin Engineering and Sciences Co., MS 303, NASA Langley Research Center, Hampton, VA 23681. Senior Member AIAA.

Q_∞^* is the dimensional freestream total velocity and ν^* is the dimensional kinematic viscosity. With $R^* = 0.114$ m, the unit Reynolds number was varied from 1.93×10^6 to $3.68 \times 10^6/\text{m}$. The sweep angle Λ was varied from $\Lambda = 53$ to 70.5 deg. The measured transition onset location varied in a range from $\theta_T^* = 40.1$ to 90.3 deg, depending on the unit Reynolds number and the sweep angle. Here, θ_T^* is the angle between the line that connects the center of the cylinder with the attachment line and the line that connects the center of the cylinder with the transition onset location line. At the same Reynolds number, an increase in Λ results in an upstream movement of the transition onset location. Furthermore, at the same Λ , an increase in the Reynolds number also results in an upstream movement of the transition onset location.

The linear stability calculations for incompressible flow over an infinite swept cylinder indicate that the correlating N factors of stationary (zero-frequency) disturbances at the experimental conditions of the 118 data points of Poll¹ vary from 3.9 to 9.4 with a mean value of 7.4. The corresponding correlating N factors of traveling disturbances vary from 11.6 to 15.7 with a mean value of 14.9. Therefore, for the same initial disturbance amplitude, the amplitude of the traveling disturbance is approximately $e^{14.9}/e^{7.4} \approx 1800$ times larger than the amplitude of a stationary disturbance. These values suggest that traveling disturbances cause transition in the experiment of Poll¹; this result is consistent with the experimental observations of Poll and is further supported by the scatter in the values of the correlating N factors. For example, the normalized standard deviation off the mean of the correlating N factors of stationary disturbances is 0.14, whereas the corresponding value for traveling disturbances is only 0.04. Note that the linear stability calculations account for the effects of body curvature and nonparallelism. The same physical wave is followed in the calculations by fixing its dimensional spanwise wave number and its dimensional frequency. Details of the mathematical formulation and methods of solution are given by Masad and Malik.²

We now analytically correlate the value of x_T with the values of Re and Λ , based on the experimental data of Poll.¹ To do so, we assume that x_T varies with Re and Λ in accordance with

$$x_T = \frac{a^2}{\Gamma_1^2 \Gamma_2^2}$$

where

$$\Gamma_1 = a_1 + (10^{-6} Re)^{a_2} \quad \Gamma_2 = b_1 + \Lambda^{b_2}$$

In these equations, a , a_1 , a_2 , b_1 , and b_2 are constant and the sweep angle Λ is in radians. The above form acknowledges the destabilizing effects of increasing the freestream Reynolds number and sweep angle. To determine the correlation constants, we minimize the sum

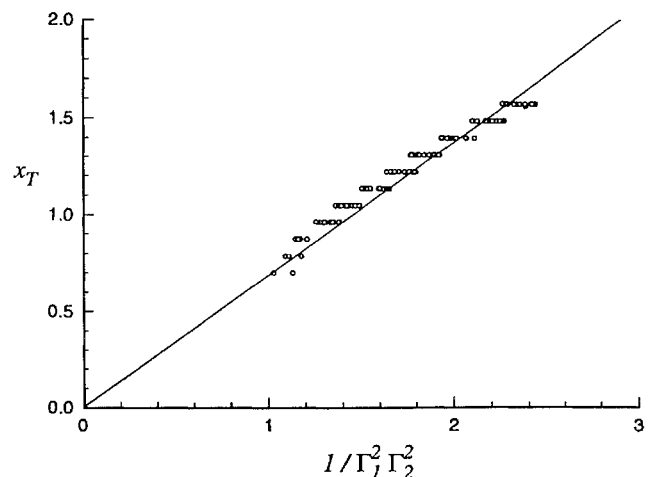


Fig. 1 Comparison between variation of correlated and actual values of transition location with correlation function.